Environmental Technology & Innovation 28 (2022) 102591

Contents lists available at ScienceDirect

Environmental Technology & Innovation

journal homepage: www.elsevier.com/locate/eti

Graphene oxide coated aluminium as an efficient antibacterial surface

P. Mandal [a], S.K. Ghosh [a,*], H.S. Grewal [b,*]

[a] Department of Physics, School of Natural Sciences, Shiv Nadar University, Gautam Buddha Nagar, Uttar Pradesh 201314, India
[b] Surface Science and Tribology Lab, Department of Mechanical Engineering, School of Engineering, Shiv Nadar University, Gautam Buddha Nagar, Uttar Pradesh 201314, India

ARTICLE INFO

Article history:
Received 31 July 2021
Received in revised form 31 January 2022
Accepted 18 April 2022
Available online 25 April 2022

Keywords:
Aluminium
Graphene oxide
Transfer method
Antibacterial activity
X-ray scattering

ABSTRACT

Antimicrobial coatings on metallic surfaces are rapidly emerging to combat bacterial pathogens. The excess use of conventional antibiotics increases the number of resistant strains at an alarming rate, which in turn leads to detrimental implications in the healthcare sector. Hence, it is of great importance in developing a new class of material with inherent bactericidal activity and good biocompatibility. In the present study, we have modified the aluminium surfaces by a coating of graphene oxide (GO) due to its excellent physicochemical properties, water dispersity and low cytotoxicity. Coatings were developed through facile and enviornment-friendly transfer method. The antimicrobial properties of GO coated aluminium are investigated against Gram-negative strain *E. coli* through agar plate counting and 'Live/Dead' fluorescence staining. Further, to shed light into the mechanism of antibacterial activity of GO at the molecular level, we have performed X-ray reflectivity (XRR) study considering a phospholipid multilayer as a model system to mimic bacteria cell membrane. Results show a significant bactericidal activity of the GO coatings compared to uncoated aluminium with lower concentration showing slightly better antibacterial property due to higher roughness. The obtained results may pave the way for engineering graphene-based antimicrobial coatings on a material surface using an easy, environment-friendly, cost-effective and straight forward processing route.

1. Introduction

Bacterial adhesion and biofilm formation on metallic components pose challenges in healthcare and many industrial applications, such as, food processing equipment, water treatment plants and ship hulls (Hasan et al., 2013; Kumar and Anand, 1998). The bacterial attachment onto these surfaces significantly limits the system performance and leads to a huge financial loss (Min et al., 2016). Among different metals, aluminium and its alloys are widely explored in industry owing to their excellent properties such as lightweight, high strength to density ratio, good corrosion resistance and excellent thermal and electrical conductivities. Aluminium and its alloys do not have any intrinsic antibacterial activity and microorganism can easily proliferate on the surface. Hence, surface coating is an effective route to modify these surfaces to extend their applications in anti-biofouling (Li et al., 2017; Wu et al., 2016). Various organic polymers, metal nanoparticles, such as, silver (Maity et al., 2016; Mollick et al., 2014a), gold (Bankura et al., 2014; Mollick et al., 2014b), zinc, copper etc. and quaternary ammonium compounds have been intensively explored as potential antibacterial coatings to limit bacterial

* Corresponding authors.
E-mail addresses: sajal.ghosh@snu.edu.in (S.K. Ghosh), harpreet.grewal@snu.edu.in (H.S. Grewal).

https://doi.org/10.1016/j.eti.2022.102591

adhesion (Druvari et al., 2018; Li et al., 2017; Sudheesh Kumar et al., 2012). However, excessive use of antibiotics, leaching of metal ions and self-aggregation of these materials are harmful to human health and environment (Jiao et al., 2017). Another approach is to prepare superhydrophobic surfaces which can significantly render bacterial growth due to their extreme de-wettability (Zhang et al., 2013). But recent studies have reported the limitation of superhydrophobic surfaces to control bacterial colonization beyond a certain threshold level (Ellinas et al., 2017). To address these issues, there is a quest for the new generation of materials that can effectively combat bacterial infections with very low cell toxicity.

Graphene-based nanomaterials are at the forefront of research since being discovered by Geim and Novoselov in 2004 (Novoselov et al., 2004). The unique physicochemical properties, such as high surface area, excellent electron mobility, strong mechanical strength, thermal conductivity, easy functionalization and remarkable biocompatibility endow the diverse range of applications of graphene from optoelectronics to the biomedical field (Cha et al., 2013; Yang et al., 2013a). The utilization of graphene derivatives has invoked enormous interest in the scientific community particularly in biological applications due to their limited toxicity towards eukaryotic cells (Rojas-Andrade et al., 2017; Zhang et al., 2010). Graphene oxide (GO) is the most commonly used graphene derivative consisting of hexagonally packed carbon atoms in a 2D crystal with oxygen functionalities on the edges and basal planes (Compton and Nguyen, 2010). Presence of these oxygen-containing groups enhances the aqueous dispersity and colloidal property of GO which facilitate its applications in biosensing (Tao et al., 2013), bioimaging (Morales-Narváez and Merkoçi, 2012), photothermal treatment (Tian et al., 2011), drug delivery (Liu et al., 2008), and as antibacterial materials (Marković et al., 2018).

In the last few years, many efforts have been devoted to investigate the antibacterial activity of graphene-based nanomaterials supported on a wide variety of substrates. Akhavan and Ghaderi (2010) have synthesized GO nanowalls on stainless steel substrates by electrophoretic deposition from a suspension of Mg^{2+}-GO nanosheets. They have concluded that the cell membrane damage of bacteria due to direct contact with the sharp edges of GO nano-walls is an effective mechanism of antibacterial activity. The reduced GO (rGO) nano-walls with enhanced sharp edges exhibited stronger antibacterial activity towards Gram-positive bacteria *S. aureus* due to lacking of the outer membrane. Hu et al. (2010) have reported the antibacterial efficiency of GO and rGO nanosheets on free-standing paper. After overnight incubation at 37 °C, no growth of Gram-negative bacteria *E. coli* on GO paper was shown, rather, there were few colonies on rGO paper, which is in contrast with the above results. On contrary, Ruiz et al. (2011) have reported that GO does not have intrinsic antibacterial activity, rather, it acts as a general enhancer of cellular growth by increasing cell attachment and proliferation. Recently, Liu et al. (2018) modified silicon (Si) rubber surface with GO coating and studied the antibacterial activity towards *E. coli* and *S. aureus*. The flat and featureless GO coated Si rubber surfaces showed enhanced antibacterial activity towards *E. coli* because of the production of oxidative stress, which is the primary reason for inhibition of bacteria cells.

The interaction of GO with bacteria membrane is not straight forward, rather, it depends on different physical properties such as flake size, thickness, concentration, presence of sharp edges and most importantly the orientation of the flakes on the deposited surface. Depending on the above parameters, a few mechanisms have already been reported in the literature including production of reactive oxygen species (Krishnamoorthy et al., 2012), oxidative stress (Hui et al., 2014), and 'insertion mode of action' which results due to direct contact of the bacteria cell membrane with sharp edges of GO (Akhavan and Ghaderi, 2010; Szunerits and Boukherroub, 2016). Even though several studies on the mechanism of antibacterial activity have been reported, the literature lacks a detailed understanding of interaction at molecular level.

In this present article, the antibacterial activity of GO coated aluminium was investigated against *E. coli* by colony-forming unit (CFU/ml) count and Live/Dead cell assay. To modify the aluminium surfaces, a facile, cost-effective and eco-friendly coating method has been employed. Due to biocompatibility and low cytotoxicity, GO was explored as an efficient antibacterial coating. The effect of different GO concentrations on antibacterial activity has been investigated. Further, a stack of phospholipid bilayers on a hydrophilic (Si) substrate has been considered as a model system to mimic the outer membrane of bacteria cell and X-ray scattering techniques have been employed to comprehend the interaction of GO with model membrane.

2. Materials and methods

2.1. Materials

Analytical grade graphite flakes (∼325 mesh, Alfa Aesar), sulfuric acid (H_2SO_4), potassium permanganate ($KMnO_4$), hydrogen peroxide (H_2O_2) [30% (v/v)], hydrochloric acid (HCl), acetone, chloroform and methanol were purchased from Fisher Scientific and used without further purification. All microbiology media and ingredients used for bacteria culture were purchased from Hi-Media, Mumbai. SYTO9 and propidium iodide (PI) stains were purchased from Thermo Fisher Scientific (UK) for Live/Dead viability assay. The neutrally charged lipid 1,2-dipalmitoyl-sn-glycero-3-phosphocholine (DPPC) was purchased from Avanti Polar Lipids (Alabaster, AL) in powder form and used to mimic bacteria cell membrane. Ultrapure Millipore water (resistivity = 18 MΩ cm) was used in all the experiments.

2.2. Synthesis and characterization of GO

Graphene oxide (GO) nano-flakes were synthesized using modified Hummer's method (Dimiev and Tour, 2014; Novoselov and Geim, 2007) which is explained briefly in supporting information (Figure S1). The synthesized GO flakes were fully characterized using different microscopic and spectroscopic techniques as shown in Figures S2 and S3.

2.3. Preparation of GO coating on Al substrate

Commercially available aluminium alloy (AA1100) of size $10 \times 10 \times 5$ mm^3 were used as substrates after polishing down to 2000 grit. The samples were cleaned ultrasonically using acetone and DI water in sequence for 15 min, followed by drying with nitrogen flow. The cleaned and dried aluminium samples were coated with GO by a simple transfer method. The Whatman filter paper (grade 540) was dipped in GO solutions of different concentrations (0.50, 1.0 and 2.0 mg/ml dispersion in DI water) and placed on top of polished aluminium samples. Then the samples were placed on a hot plate at 110 °C for 5–10 min. The filter paper was naturally peeled off leaving a pure coating of GO onto the surfaces. This process was repeated 2–3 times to obtain a uniform coating. Then the samples were stored at 50 °C for further use.

2.4. Characterization

The surface morphology of GO coated aluminium samples were investigated using field emission scanning electron microscope, FESEM (Nova Nano SEM 450, FEI, Netherlands) via energy dispersive spectroscopy (EDS) and atomic force microscopy, AFM (XE7, Park system). To confirm the chemical composition of coated surfaces, X-ray photoelectron spectroscopy (XPS) measurements were carried out in an Omicron Multiprobe Surface Analysis System using a monochromatized AlK α (1486.7 eV) radiation source. The water contact angles of unprocessed and coated samples were measured in a contact angle measurement system (Apex, Kolkata) using a water droplet of volume 5 μl. The adhesion of the coating has been confirmed by sonication test with varying time followed by measuring the contact angle. The reported values are the average of at least four measurements at different places of the samples. The error bar indicates the standard deviation value. All measurements were performed at room temperature.

2.5. Antibacterial activity

2.5.1. Bacterial strains and culture condition

Antibacterial activity of the GO coated surfaces was tested using *Escherichia coli* (*E. coli, DH5, alpha*) as a representative Gram-negative bacteria strain. A single colony of *E. coli* was collected from glycerol stock and incubated overnight at 37 °C in 5 ml LB broth to prepare primary culture. The cultured suspension was centrifuged and washed using 1X PBS buffer to remove surplus macromolecules and re-suspended in saline solution to adjust optical density $(OD)_{600}$ $\sim$0.2.

2.5.2. Cell viability of GO coated aluminium surfaces

The unprocessed (control) and GO coated aluminium surfaces used for antibacterial activity were first sterilized to avoid any contaminations. Then the samples were placed in a sterile 12-well plate and 100 μl aliquots of bacteria culture were added on top of the surfaces. Then the samples were incubated at 37 °C for different time intervals. During incubation, wet tissue papers were used inside the 12-well plate to minimize the evaporation of the bacteria culture. After a certain time interval, the cell suspension was pipetted out from the samples and diluted serially to get spot assays and colony-forming units (CFU). 100 μl of diluted culture was spread on a nutrient agar plate and incubated overnight at 37 °C in static condition. Then the number of colonies was counted. The experiment was repeated for three different sets of samples.

2.5.3. Live/Dead cell assay

The viability of bacteria attached to the GO coated surfaces was studied using a Live/Dead cell assay kit. A mixture of 2.5 μM SYTO9 and 15 μM propidium iodide (PI) were prepared in saline solution according to the manufacture's instruction (Stiefel et al., 2015) and used to stain the bacterial cells. The treated cells were centrifuged and the pellet was washed thoroughly using 1X PBS solution and re-suspended with saline solution. 3 μl of the dye mixture was added to the solution and incubated in the dark for 15 min at room temperature. Then the cells were again washed 2–3 times and re-suspended in 100 μl saline solution. Stained cells were observed under fluorescence microscopy (Nikon Eclipse Ti) equipped with Nikon DS-U3 camera using Plan Apo 100X/1.40 oil objective.

2.6. X-ray reflectivity (XRR) study of model cell membrane

The stacked bilayers of zwitterionic phospholipid, DPPC, on a hydrophilic Si substrate was used to mimic the cellular membrane of bacteria. To prepare the lipid multilayers, small pieces of Si substrates were cleaned ultrasonically using methanol and DI water followed by drying in a nitrogen flow. Then the substrates were exposed to UV radiation for 20 min at 25 °C to make it hydrophilic for uniform deposition. The stock solution of lipid (5 mg/ml) was prepared in chloroform while the GO flakes were dissolved in DI water. A particular wt. % of GO was added to the lipid solution and vortexed to obtain a uniform solution. 60–70 μL of the solutions were dropped cast on cleaned Si substrates and left inside a fume hood for the evaporation of the solvent. Then the samples were placed in a vacuum oven overnight to remove the remaining traces of solvents. Then the samples were kept in an oven at 50 °C for 24 h in a saturated salt solution environment to reach a particular relative humidity (RH). The samples were then sealed in a custom-designed

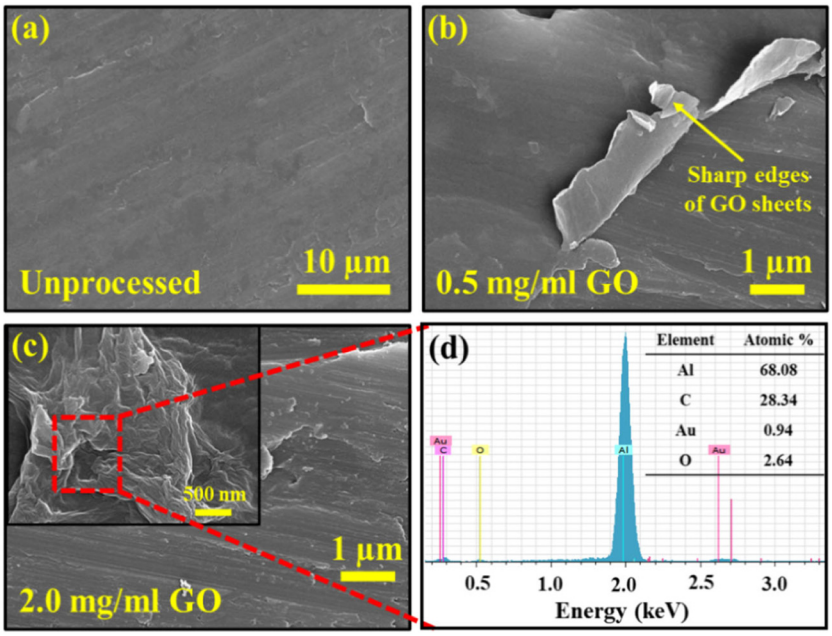

Fig. 1. FESEM micrographs of (a) unprocessed aluminium, (b) 0.5 mg/ml GO coating, (c) 2.0 mg/ml GO coating, (d) EDS spectra of 2.0 mg/ml GO coated aluminium.

closed sample chamber for reflectivity measurements at a particular RH inside the chamber controlled by a saturated salt solution (Ma et al., 2016).

The X-ray reflectivity (XRR) measurements were carried out in an in-house reflectometer (Bruker, D8 discover) using the monochromatic source of energy 8 keV (Cu Kα radiation, $\lambda = 1.542$ Å). The beam was aligned and collimated to a size of 0.2(h) $\times$ 1(v) mm. The XRR data were recorded as a function of incident angle from 0 to 6° with a step size of 0.025°.

3. Results and discussions

3.1. Characterization of GO coated aluminium

3.1.1. Surface morphology

The FESEM images illustrating the surface structure of unprocessed and GO coated aluminium surfaces with different concentrations are shown in Fig. 1. Fig. 1(a) represents the morphology of freshly polished aluminium, which shows overall a smooth surface except for a few polishing marks. Fig. 1(b) and (c) exhibit formation of layered structure throughout the surface with wrinkle-like morphology. The images also show sharp edges of GO sheets protruding out due to the stacking of multiple layers. The random orientation of GO sheets was observed for coating with 0.5 mg/ml whereas, for higher concentration (2.0 mg/ml), relatively smooth morphology was noticed. The thickness of the coating was measured to be 63 $\pm$ 3 nm for 0.5 mg/ml coating and 283 $\pm$ 8 nm for 2.0 mg/ml GO coating (Figure S4). This could be due to a higher fraction of GO sheets resulting in significant superimposition of sheets with a smoothening effect, which agrees well with the parameters obtained from AFM imaging (Figure S5). The average roughness of 0.5 mg/ml coating is found to be 54 $\pm$ 2 nm and decreased to 21 $\pm$ 2 nm for 2 mg/ml coating, which again confirms the smooth morphology at higher concentration.

3.1.2. Chemical composition

The GO coated aluminium surfaces are analysed by energy dispersive spectroscopy (EDS) and X-ray photoelectron spectroscopy (XPS) to confirm the chemical states of different elements. The EDS spectra (Fig. 1(d)) and XPS wide survey scan (Fig. 2(a)) both confirm the presence of C and O with a negligible amount of sulphur. For quantitative analysis, two major peaks, C-1s and O-1s are de-convoluted using Voigt function after Shirley type background subtraction using CASA-XPS processing software which is shown in Fig. 2(b) and (c). The de-convoluted C-1s peak centered at binding energies of 286.5, 288.2 and 288.8 eV correspond to C–OH, C=O and COOH functional groups, respectively along with C=C/C–C rich domains at ~284.5 eV. The relative percentages of C=C/C–C, C–OH, C=O and COOH groups are calculated from de-convoluted peaks and found to be 53, 40, 4 and 3%, respectively which is in agreement with previous report (Al-Gaashani et al., 2019). The deconvoluted O-1s peak centered at binding energies of 531.1 and 532.3 eV attributed to C–C

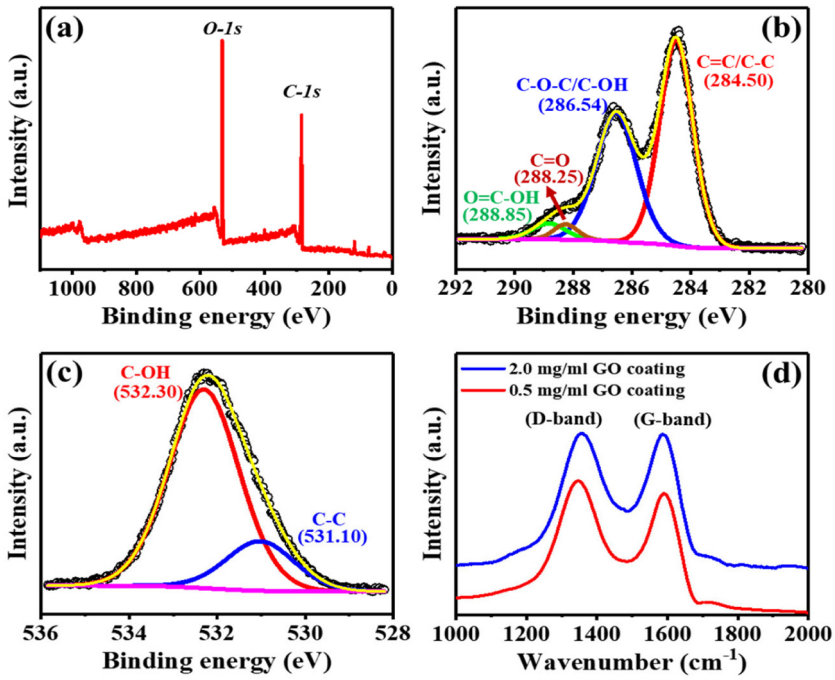

Fig. 2. (a) X-ray photoelectron spectra (survey scan), (b) high resolution de-convoluted C-1s spectra, (c) de-convoluted O-1s spectra, (d) Raman spectra of GO coated aluminium.

and C–OH groups respectively. These de-convoluted peaks confirm that GO coated aluminium possess highly oxygenated functionalities.

The chemical composition of the coating is further studied by Raman spectroscopy. For GO coated aluminium, the typical D and G bands appear at 1358 cm^{-1} and 1587 cm^{-1}, respectively and the intensity ratio is $I_D/I_G = 1.01$ (Fig. 2(d)). The G peak is related to the first-order scattering of E_{2g} phonon of sp^2 carbon and the D peak arises due to A_{1g} symmetry corresponds to the disorder/defect states. The intensity ratio of these two bands generally indicates the quality of the sample. Compare to pristine GO (Figure S2(b)), the coated samples possess a slightly higher intensity ratio which indicates the presence of structural defects (Johra et al., 2014).

3.2. Surface wettability and coating adhesion

Surface roughness and chemical composition play an important role in controlling the wetting behaviour of any materials, which, in turn, also influence the antibacterial activity of the surface. The polished unprocessed aluminium is nearly hydrophobic with a static contact angle (SA) of 81° ± 3°. After GO coating, the surfaces showed increased wettability. For 0.5 mg/ml GO coating, the SA reduces to 65° ± 2°, whereas it reduces to 56° ± 2° for 2.0 mg/ml GO coating (Fig. 3(a)). As is evident from FESEM images (Fig. 1(b) and (c)), coating of GO at lower concentration have produced sharp edges of the flakes, whereas, for higher concentration, it is almost smooth which also influences the wetting behaviour of the coated samples. As measured from AFM studies (Figure S4), the roughness factor for 0.5 and 2.0 mg/ml GO coating is found to be 1.10 and 1.06, whereas the average roughness is 54 ± 2 nm and 21 ± 2 nm respectively. With the varying concentration of GO, a small change in wettability of aluminium surface can be explained depending on the hydrophilicity of GO sheets. With increasing concentration, the number of oxygen functionalities on the surface increases promoting the interaction with water which lowers the contact angle.

Further, the adhesion of the coating with substrates is a prime factor that determines the system performance in harsh environments. The adhesion of this coating was examined as a function of sonication time which is shown in Fig. 3(b). From CA measurement it is clear that there is no significant effect on surface wettability after 5 min sonication in an ultrasonic bath which confirms the good adhesion of the coating with aluminium surface. As the coating method was repeated 2–3 times for uniform coverage and heated at 110 °C, it enhances the intimate contact and the bonding with metal surfaces. A mild decrease in contact angle for 2.0 mg/ml concentration coating was observed which could be due to minor delamination of GO sheets.

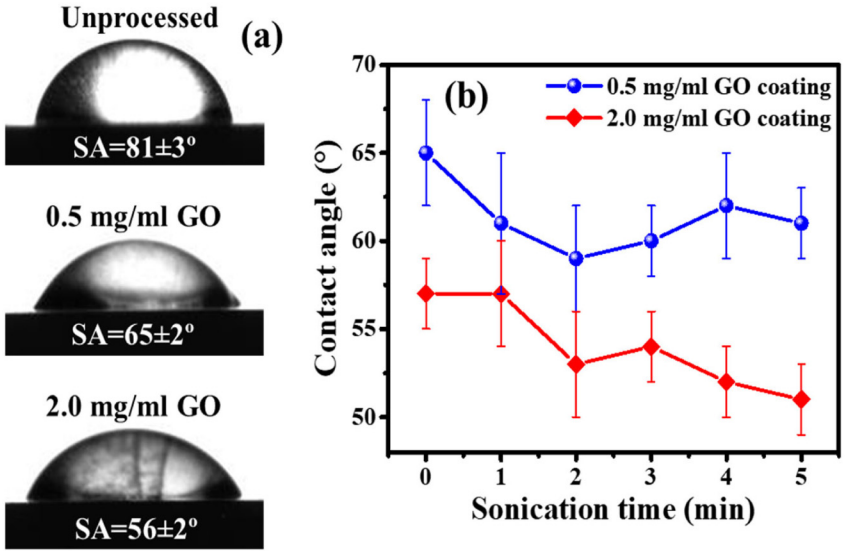

Fig. 3. (a) Wettability of unprocessed and GO coated aluminium surfaces with different concentrations. (b) The durability of the coating has been checked as a function of sonication time. SA: Static contact angle.

3.3. Antibacterial activity of GO coated aluminium

The antibacterial activity of graphene-based nanomaterials are well established and a plethora of studies have already been reported in the literature. Most of these studies mainly focus on dispersed GO nano-sheets in suspension. The present work is an effort to fabricate GO coated metallic surfaces to prevent bacterial adhesion and biofilm formation. These surfaces are important for the development of nontoxic coating in biomedical applications. The antibacterial activity of GO coated aluminium surfaces are evaluated using spot assay and plate counting method against Gram-negative bacteria *E. coli*. To have a benchmark, the unprocessed aluminium sample is used as a control. Fig. 4(a) shows the CFU/ml data for unprocessed and GO coated aluminium along with the images of petri plates which is shown in Fig. 4(b). For the control sample, no considerable antibacterial activity is observed till 4 h of incubation as the number of colony forming units (CFU) increases steadily. However, the GO coated aluminium exhibits significant bactericidal activity even after 2 h of incubation. A drastic reduction in the CFU is observed for 0.5 mg/ml GO coating after 4 h incubation. Only a few colonies are observed on 2.0 mg/ml GO coated surfaces. There is a slight variation in the inhibition efficiency of GO coating with different concentrations. The sharp edges of GO sheet at lower concentrations are found to be more lethal to bacteria cells in comparison to higher concentrations. The wettability of the coating does not play significant role in controlling antibacterial activity of GO coating.

To get more insights into the bactericidal effect of GO coated surfaces, Live/Dead assay has been employed. Here, a mixture of two fluorescent dyes, SYTO9 and propidium iodide (PI) are used to stain the treated bacteria cells. SYTO9 can permeate into both the live and dead cells and bind to DNA to give rise the green fluorescence. The PI only enters through the damaged membrane of cells and gives red fluorescence. Therefore, in fluorescence image, the live cells are indicated as green and the dead cells are represented as red with a compromised cell membrane (Choudhary and Das, 2019). Fig. 5 shows the fluorescence image of stained bacteria on unprocessed and GO coated aluminium surfaces. The cells incubated on unprocessed aluminium gives green fluorescence depicting all the cells to be alive. In contrary, the GO coated surfaces show red fluorescence confirming nearly all the cells to be dead. Besides, 0.5 mg/ml GO coating exhibits stronger antibacterial activity compared to 2.0 mg/ml GO coating which is in good agreement with the CFU counts. The results suggest that the GO coating on aluminium surface-induces irreversible membrane damage, which may cause the cell to die.

3.4. Mechanism of antibacterial activity of GO coated aluminium: X-ray reflectivity study

In the section above, it has been shown that the damage of cellular membrane may cause the bacterial death. As there is not much reports on the molecular description of this damage, a detailed structural picture is required to understand and control the antibacterial activity of graphene-based nano materials. Only qualitative explanations including penetration of sharp edges of GO into cell membrane, production of reactive oxygen species and oxidative stress are reported in literature (Perreault et al., 2015a; Yang et al., 2013b). Nevertheless, a few computer simulation studies have reported

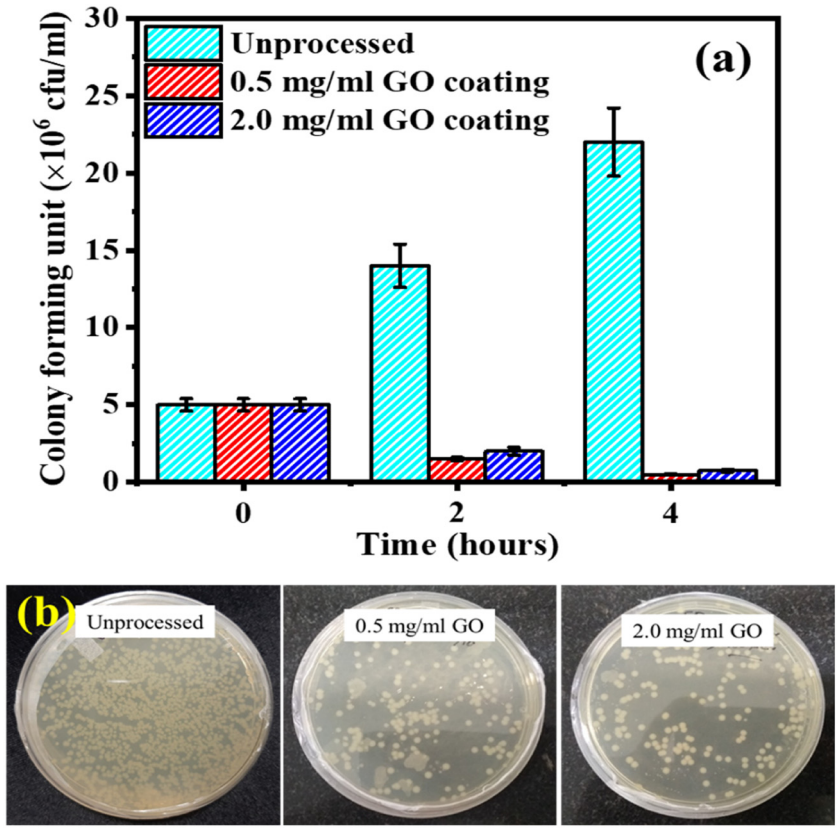

Fig. 4. Antibacterial activity of unprocessed and GO coated aluminium surfaces: (a) colony forming units (CFU)/ml as a function of time. E. coli bacterial growth significantly reduced for GO coated aluminium surfaces and (b) photographs of petri plates used to calculate CFU/ml.

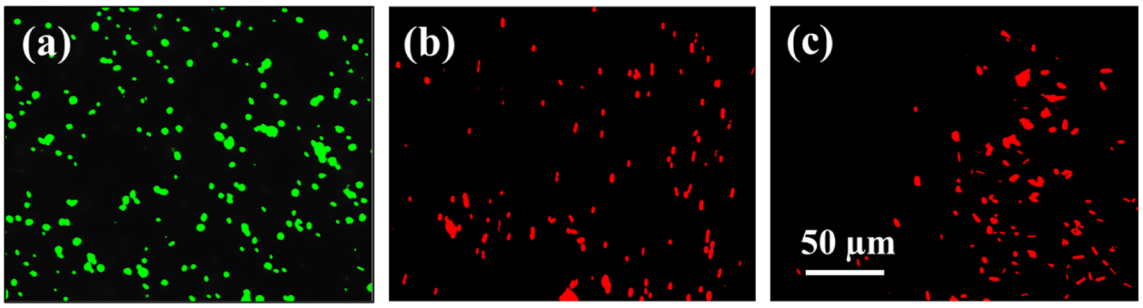

Fig. 5. Fluorescence microscope images of Gram-negative bacteria cell E. coli after 12 h incubation on unprocessed and GO coated aluminium substrates. (a) unprocessed, (b) 0.5 mg/ml GO coated and (c) 2.0 mg/ml GO coated aluminium. E. coli was exposed to SYTO9 as green fluorescent and PI as red fluorescent. The scale bar is 50 µm. (For interpretation of the references to colour in this figure legend, the reader is referred to the web version of this article.)

different possible interactions of GO in lipid membrane (Li et al., 2013; Tu et al., 2013). Chen et al. (2016) have reported that graphene can easily penetrate into the lipid membrane due to hydrophobic interaction with lipid tails and extract a large amount of phospholipids from the membrane while the penetration of GO highly depends on their size, oxidation level and initial orientation to the phospholipid membrane.

In our simplistic model, cellular membrane is mimicked with multiple layers of a zwitterionic phospholipid membranes on a Si-substrate and X-ray scattering studies have been performed. Such a multilayer sample has been considered to obtain the X-ray diffraction peaks from one-dimensional organization of the bilayers along the substrate normal. Fig. 6 represents the XRR data obtained from the DPPC and DPPC/GO composite with different wt. % of added GO. The XRR profile of pure DPPC consists of a single set of equidistant (q_{z_1}: q_{z_2}: q_{z_3}: ... = 1: 2: 3: ...) Bragg peaks obtained due to the one-dimensional periodicity confirming a homogeneous lamellar phase. Interestingly, presence of GO indicates the

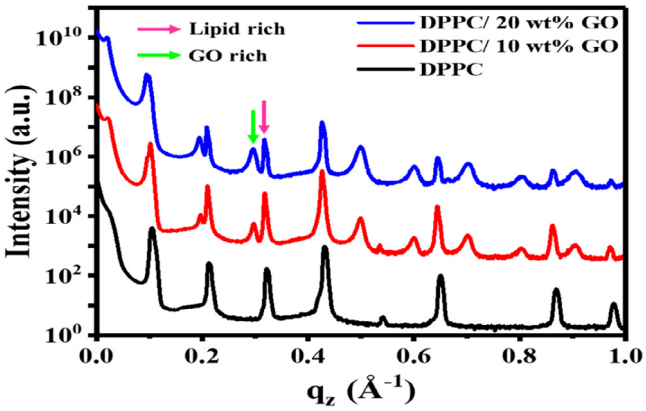

Fig. 6. X-ray reflectivity (XRR) pattern of DPPC multilayers on a Si substrate with different wt. % of added GO.

appearance of two distinct sets of equidistance diffraction peaks which arise due to coexistence of two lamellar phases in the samples. One lamellar phase can be denoted as *lipid-rich* phase as the *d*-spacing and shape of Bragg peaks are similar to that of the pure lipid phase. The other phase has been denoted as *GO-rich* phase which arises at lower value of q_z with a distinctly different shape of Bragg peaks. The *d-spacing* for pure DPPC is calculated to be 59.7 Å which is increased to 63.5 Å at 20% of added GO. For the new set of peaks corresponding to *GO-rich* phase shows an increase of about 7 Å at the same concentration of GO. At the same time, the Bragg peaks become broad in presence of GO with a modified intensity suggesting a disordering effect in the system as well as an increase in interfacial roughness (Jing et al., 2009). From the above results we can conclude that the presence of GO flakes brings a significant structural change in the cell membrane. The interaction of GO with zwitterionic phospholipid membrane results from the balance of multiple forces. The GO flakes are enriched with carboxyl groups (COO^-) at the edges which provide an electrostatic attraction with positively charged choline moiety of lipid heads. In that case, the flakes are supposed to be attached to head groups lying above the membrane (*lipid-rich* phase). Further, as only 30% of atoms are oxidized in the synthesized GO, there are huge intact graphitic domain of GO which experiences a hydrophobic interaction with lipid tails triggering the insertion of GO into the membrane (*GO-rich* phase). The above-mentioned mechanism is pictorially represented in Fig. 7 showing the adsorption of GO sheets into the lipid membrane. A more detailed molecular description of these *lipid-rich* and *GO-rich* phases can be found in our recent publication (Mandal et al., 2021a). The zeta potential of GO-flakes is measured to be negative (−52 mV for 0.5 mg/ml) due to presence of electronegative functional groups. The outer membrane of *E-Coli* is composed of phospholipids with either permanent dipole moment or negatively charged head groups. Therefore, electrostatics play a vital role in the GO-membrane interaction. In our recent study (Mandal et al., 2021b), we have shown the charge dependent interaction of GO with model cellular membrane using differently charged phospholipid monolayer at air–water interface. The results show a strong interaction with positively charged lipids, a weak interaction with zwitterionic lipids and negligible interaction with negatively charged lipids.

The cellular membrane is a self-assembled structure of various lipids where other macromolecules such as proteins, cholesterols are embedded (Cooper, 2000; Van Meer et al., 2008). This membrane is not only the protective boundary of a cell but it also plays roles in many other activities including cell signalling, exocytosis–endocytosis process etc. (Sigismund et al., 2012). Any structural perturbation here can cause the membrane to malfunction. As explained above and given in Fig. 7, the distorted and disordered structure of cell membrane induced by the GO-flakes probably causes the bacteria to die leading to the bactericidal property of GO-coated metallic surface. These results are in well agreement with the previous findings where deformation and alteration of cell morphology was reported as the driving mechanism for antibacterial activity of GO coated surfaces (Chen et al., 2014; Hu et al., 2010; Perreault et al., 2015b).

4. Conclusions

This work concludes the successful synthesis, characterization and highly adhesive coatings of GO on aluminium substrates through a simple transfer method. The coated surfaces are characterized using FESEM, EDS, XPS and Raman spectroscopy. Both the colony-forming unit and fluorescence staining tests confirm the excellent antibacterial activity of GO coated surfaces as compared to unprocessed aluminium. Further, XRR results confirm the adsorption of GO sheets into phospholipid layer which can perturb membrane structure and significantly reduce cell viability. Present findings pave the way of designing graphene-based antibacterial coating on substrates using an easy, cost-effective and environment-friendly processing route.

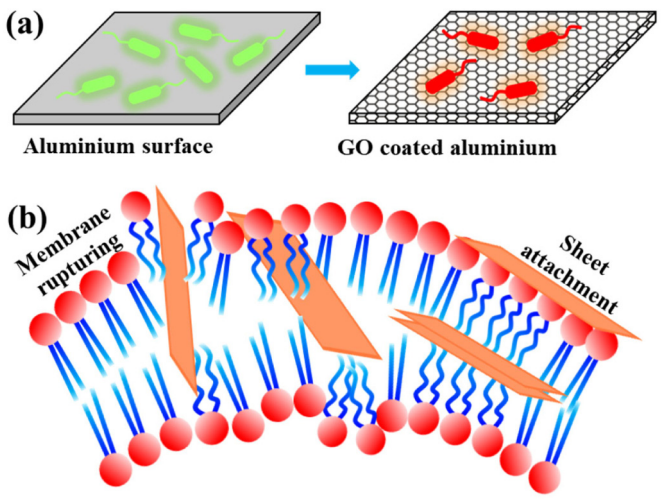

Fig. 7. (a) Schematic representation of antibacterial activity of unprocessed and GO coated aluminium surfaces. (b) Mechanism of interaction of graphene oxide with cellular membrane that rupture the cell by attaching and penetrating into the membrane heads.

CRediT authorship contribution statement

P. Mandal: Methodology, Validation, Investigation, Visualization, Writing – original draft. **S.K. Ghosh:** Conceptualization, Methodology, Resources, Writing – review & editing. **H.S. Grewal:** Conceptualization, Methodology, Supervision, Resources, Writing – review & editing.

Declaration of competing interest

The authors declare that they have no known competing financial interests or personal relationships that could have appeared to influence the work reported in this paper.

Acknowledgements

P. M. is thankful to SNU for the PhD fellowship. H. S. G. acknowledges the financial assistance provided by Council of Scientific and Industrial Research (CSIR), India, under the project title "Development of Durable Self-Cleaning Surfaces", (Grant No. 22/0756/17/EMR-II). S. K. G. acknowledges the financial support provided by Science & Engineering Research Board (SERB), India, Department of Science and Technology (DST), India for funding this project (File no. EMR/20l6/006221). We are thankful to Mr. Ajit Seth for his help in FESEM imaging and Ms. Rashmi Niranjan for her help in taking fluorescence images.

Appendix A. Supplementary data

Supplementary material related to this article can be found online at https://doi.org/10.1016/j.eti.2022.102591.

References

Akhavan, O., Ghaderi, E., 2010. Toxicity of graphene and graphene oxide nanowalls against bacteria. ACS Nano 4 (10), 5731–5736.
Al-Gaashani, R., Najjar, A., Zakaria, Y., Mansour, S., Atieh, M., 2019. XPS and structural studies of high quality graphene oxide and reduced graphene oxide prepared by different chemical oxidation methods. Ceram. Int. 45 (11), 14439–14448.
Bankura, K., Maity, D., Mollick, M.M.R., Mondal, D., Bhowmick, B., Roy, I., Midya, T., Sarkar, J., Rana, D., Acharya, K., 2014. Antibacterial activity of Ag–Au alloy NPs and chemical sensor property of Au NPs synthesized by dextran. Carbohydr. Polymers 107, 151–157.
Cha, C., Shin, S.R., Annabi, N., Dokmeci, M.R., Khademhosseini, A., 2013. Carbon-based nanomaterials: multifunctional materials for biomedical engineering. ACS Nano 7 (4), 2891–2897.
Chen, J., Peng, H., Wang, X., Shao, F., Yuan, Z., Han, H., 2014. Graphene oxide exhibits broad-spectrum antimicrobial activity against bacterial phytopathogens and fungal conidia by intertwining and membrane perturbation. Nanoscale 6 (3), 1879–1889.
Chen, J., Zhou, G., Chen, L., Wang, Y., Wang, X., Zeng, S., 2016. Interaction of graphene and its oxide with lipid membrane: a molecular dynamics simulation study. J. Phys. Chem. C 120 (11), 6225–6231.
Choudhary, P., Das, S.K., 2019. Bio-reduced graphene oxide as a nanoscale antimicrobial coating for medical devices. ACS Omega 4 (1), 387–397.
Compton, O.C., Nguyen, S.T., 2010. Graphene oxide, highly reduced graphene oxide, and graphene: versatile building blocks for carbon-based materials. Small 6 (6), 711–723.
Cooper, G.M., 2000. The Cell: A Molecular Approach, second ed. Sinauer Associates.

Dimiev, A.M., Tour, J.M., 2014. Mechanism of graphene oxide formation. ACS Nano 8 (3), 3060–3068.
Druvari, D., Koromilas, N.D., Bekiari, V., Bokias, G., Kallitsis, J.K., 2018. Polymeric antimicrobial coatings based on quaternary ammonium compounds. Coatings 8 (1), 8.
Ellinas, K., Kefallinou, D., Stamatakis, K., Gogolides, E., Tserepi, A., 2017. Is there a threshold in the antibacterial action of superhydrophobic surfaces? ACS Appl. Mater. Interfaces 9 (45), 39781–39789.
Hasan, J., Crawford, R.J., Ivanova, E.P., 2013. Antibacterial surfaces: the quest for a new generation of biomaterials. Trends Biotechnol. 31 (5), 295–304.
Hu, W., Peng, C., Luo, W., Lv, M., Li, X., Li, D., Huang, Q., Fan, C., 2010. Graphene-based antibacterial paper. ACS Nano 4 (7), 4317–4323.
Hui, L., Piao, J.-G., Auletta, J., Hu, K., Zhu, Y., Meyer, T., Liu, H., Yang, L., 2014. Availability of the basal planes of graphene oxide determines whether it is antibacterial. ACS Appl. Mater. Interfaces 6 (15), 13183–13190.
Jiao, Y., Niu, L.-n., Ma, S., Li, J., Tay, F.R., Chen, J.-h., 2017. Quaternary ammonium-based biomedical materials: State-of-the-art, toxicological aspects and antimicrobial resistance. Prog. Polym. Sci. 71, 53–90.
Jing, H., Hong, D., Kwak, B., Choi, D., Shin, K., Yu, C.-J., Kim, J., Noh, D., Seo, Y., 2009. X-ray reflectivity study on the structure and phase stability of mixed phospholipid multilayers. Langmuir 25 (7), 4198–4202.
Johra, F.T., Lee, J.-W., Jung, W.-G., 2014. Facile and safe graphene preparation on solution based platform. J. Ind. Eng. Chem. 20 (5), 2883–2887.
Krishnamoorthy, K., Veerapandian, M., Zhang, L.-H., Yun, K., Kim, S.J., 2012. Antibacterial efficiency of graphene nanosheets against pathogenic bacteria via lipid peroxidation. J. Phys. Chem. C 116 (32), 17280–17287.
Kumar, C.G., Anand, S.K., 1998. Significance of microbial biofilms in food industry: a review. Int. J. Food Microbiol. 42 (1–2), 9–27.
Li, M., Mitra, D., Kang, E.-T., Lau, T., Chiong, E., Neoh, K.G., 2017. Thiol-ol chemistry for grafting of natural polymers to form highly stable and efficacious antibacterial coatings. ACS Appl. Mater. Interfaces 9 (2), 1847–1857.
Li, Y., Yuan, H., Von Dem Bussche, A., Creighton, M., Hurt, R.H., Kane, A.B., Gao, H., 2013. Graphene microsheets enter cells through spontaneous membrane penetration at edge asperities and corner sites. Proc. Natl. Acad. Sci. 110 (30), 12295–12300.
Liu, Z., Robinson, J.T., Sun, X., Dai, H., 2008. PEGylated nanographene oxide for delivery of water-insoluble cancer drugs. J. Am. Chem. Soc. 130 (33), 10876–10877.
Liu, Y., Wen, J., Gao, Y., Li, T., Wang, H., Yan, H., Niu, B., Guo, R., 2018. Antibacterial graphene oxide coatings on polymer substrate. Appl. Surf. Sci. 436, 624–630.
Ma, Y., Ghosh, S.K., DiLena, D.A., Bera, S., Lurio, L.B., Parikh, A.N., Sinha, S.K., 2016. Cholesterol partition and condensing effect in phase-separated ternary mixture lipid multilayers. Biophys. J. 110 (6), 1355–1366.
Maity, D., Pattanayak, S., Mollick, M.M.R., Rana, D., Mondal, D., Bhowmick, B., Dash, S.K., Chattopadhyay, S., Das, B., Roy, S., 2016. Green one step morphosynthesis of silver nanoparticles and their antibacterial and anticancerous activities. New J. Chem. 40 (3), 2749–2762.
Mandal, P., Bhattacharya, G., Bhattacharyya, A., Roy, S.S., Ghosh, S.K., 2021a. Unravelling the structural changes of phospholipid membranes in presence of graphene oxide. Appl. Surf. Sci. 539, 148252.
Mandal, P., Giri, R.P., Murphy, B.M., Ghosh, S.K., 2021b. Self-assembly of graphene oxide nanoflakes in a lipid monolayer at the air–water interface. ACS Appl. Mater. Interfaces 13 (48), 57023–57035.
Marković, Z.M., Jovanović, S.P., Mašković, P.Z., Danko, M., Mičušík, M., Pavlović, V.B., Milivojević, D.D., Kleinová, A., Špitalský, Z., Marković, B.M.T., 2018. Photo-induced antibacterial activity of four graphene based nanomaterials on a wide range of bacteria. Rsc Adv. 8 (55), 31337–31347.
Min, J., Choi, K.Y., Dreaden, E.C., Padera, R.F., Braatz, R.D., Spector, M., Hammond, P.T., 2016. Designer dual therapy nanolayered implant coatings eradicate biofilms and accelerate bone tissue repair. ACS Nano 10 (4), 4441–4450.
Mollick, M.M.R., Bhowmick, B., Maity, D., Mondal, D., Roy, I., Sarkar, J., Rana, D., Acharya, K., Chattopadhyay, S., Chattopadhyay, D., 2014a. Green synthesis of silver nanoparticles-based nanofluids and investigation of their antimicrobial activities. Microfluid. Nanofluid. 16 (3), 541–551.
Mollick, M.M.R., Bhowmick, B., Mondal, D., Maity, D., Rana, D., Dash, S.K., Chattopadhyay, S., Roy, S., Sarkar, J., Acharya, K., 2014b. Anticancer (*in vitro*) and antimicrobial effect of gold nanoparticles synthesized using *Abelmoschus esculentus* (L.) pulp extract via a green route. RSC Adv. 4 (71), 37838–37848.
Morales-Narváez, E., Merkoçi, A., 2012. Graphene oxide as an optical biosensing platform. Adv. Mater. 24 (25), 3298–3308.
Novoselov, K.S., Geim, A., 2007. The rise of graphene. Nature Mater. 6 (3), 183–191.
Novoselov, K.S., Geim, A.K., Morozov, S.V., Jiang, D., Zhang, Y., Dubonos, S.V., Grigorieva, I.V., Firsov, A.A., 2004. Electric field effect in atomically thin carbon films. Science 306 (5696), 666–669.
Perreault, F., De Faria, A.F., Elimelech, M., 2015a. Environmental applications of graphene-based nanomaterials. Chem. Soc. Rev. 44 (16), 5861–5896.
Perreault, F., De Faria, A.F., Nejati, S., Elimelech, M., 2015b. Antimicrobial properties of graphene oxide nanosheets: why size matters. ACS Nano 9 (7), 7226–7236.
Rojas-Andrade, M.D., Chata, G., Rouholiman, D., Liu, J., Saltikov, C., Chen, S., 2017. Antibacterial mechanisms of graphene-based composite nanomaterials. Nanoscale 9 (3), 994–1006.
Ruiz, O.N., Fernando, K.S., Wang, B., Brown, N.A., Luo, P.G., McNamara, N.D., Vangsness, M., Sun, Y.-P., Bunker, C.E., 2011. Graphene oxide: a nonspecific enhancer of cellular growth. ACS Nano 5 (10), 8100–8107.
Sigismund, S., Confalonieri, S., Ciliberto, A., Polo, S., Scita, G., Di Fiore, P.P., 2012. Endocytosis and signaling: cell logistics shape the eukaryotic cell plan. Physiol. Rev. 92 (1), 273–366.
Stiefel, P., Schmidt-Emrich, S., Maniura-Weber, K., Ren, Q., 2015. Critical aspects of using bacterial cell viability assays with the fluorophores SYTO9 and propidium iodide. BMC Microbiol. 15 (1), 36.
Sudheesh Kumar, P., Lakshmanan, V.-K., Anilkumar, T., Ramya, C., Reshmi, P., Unnikrishnan, A., Nair, S.V., Jayakumar, R., 2012. Flexible and microporous chitosan hydrogel/nano ZnO composite bandages for wound dressing: in vitro and in vivo evaluation. ACS Appl. Mater. Interfaces 4 (5), 2618–2629.
Szunerits, S., Boukherroub, R., 2016. Antibacterial activity of graphene-based materials. J. Mater. Chem. B 4 (43), 6892–6912.
Tao, Y., Lin, Y., Huang, Z., Ren, J., Qu, X., 2013. Incorporating graphene oxide and gold nanoclusters: A synergistic catalyst with surprisingly high peroxidase-like activity over a broad pH range and its application for cancer cell detection. Adv. Mater. 25 (18), 2594–2599.
Tian, B., Wang, C., Zhang, S., Feng, L., Liu, Z., 2011. Photothermally enhanced photodynamic therapy delivered by nano-graphene oxide. ACS Nano 5 (9), 7000–7009.
Tu, Y., Lv, M., Xiu, P., Huynh, T., Zhang, M., Castelli, M., Liu, Z., Huang, Q., Fan, C., Fang, H., 2013. Destructive extraction of phospholipids from *Escherichia coli* membranes by graphene nanosheets. Nature Nanotechnol. 8 (8), 594.
Van Meer, G., Voelker, D.R., Feigenson, G.W., 2008. Membrane lipids: where they are and how they behave. Nat. Rev. Mol. Cell Biol. 9 (2), 112–124.
Wu, M., Ma, B., Pan, T., Chen, S., Sun, J., 2016. Silver-nanoparticle-colored cotton fabrics with tunable colors and durable antibacterial and self-healing superhydrophobic properties. Adv. Funct. Mater. 26 (4), 569–576.
Yang, Y., Asiri, A.M., Tang, Z., Du, D., Lin, Y., 2013a. Graphene based materials for biomedical applications. Mater. Today 16 (10), 365–373.
Yang, K., Li, Y., Tan, X., Peng, R., Liu, Z., 2013b. Behavior and toxicity of graphene and its functionalized derivatives in biological systems. Small 9 (9–10), 1492–1503.
Zhang, Y., Ali, S.F., Dervishi, E., Xu, Y., Li, Z., Casciano, D., Biris, A.S., 2010. Cytotoxicity effects of graphene and single-wall carbon nanotubes in neural phaeochromocytoma-derived PC12 cells. ACS Nano 4 (6), 3181–3186.
Zhang, X., Wang, L., Levänen, E., 2013. Superhydrophobic surfaces for the reduction of bacterial adhesion. Rsc Adv. 3 (30), 12003–12020.